INVESTIGATION OF THERMOSYPHON LOOP PERFORMANCE IN DOUBLE-CYCLE DISTILLATION HEAT PUMP SYSTEM

Mohammed A. Hussien
Assistant Lecturer
Automobile Department-Najaf Technical College

ABSTRACT

The performance of a thermosyphon loop in a double – cycle distillation heat pump system, utilizing water as a working fluid and finned tube heat exchangers for evaporator and condenser, has been investigated. A mathematical model is set for the whole system and a simulating program is developed to simulate the double – cycle processes during the steady – state operation. A complete steam tables subroutine developed and incorporated with the main program to calculate the water and steam properties in the range of (60 – 120)^{o} C and (0.199 – 1.985)bar. The experimental results show good agreement with the results obtained from the computer program (Quick Basic). During steady – state operation of the system, it found that the thermosyphon loop performance (loop conductance) increase when the working mass flow rate increase and also it increase when the working fluid pressure increase and has a maximum value (493.022 W/m^{2}. K) At working mass flow rate of 5.5 kg/hr, working fluid pressure of 0.8 bar and process fluid pressure of 1.01825 bar.

KEYWORDS: Thermosyphon Loop, Double-cycle, Distillation, heat pump, Performance

دراسة اداء دورة سايفون حراري في مضخة حرارية لمنظومة تقطير ثنائية الدورة

محمد عبدالرضا حسين
الكليه التقنيه النجف

الخلاصة

تم دراسة اداء دورة سيفون حراري في مضخة حرارية ثنائية الدورة باستخدام الماء كسائل عمل و مبادلات حرارية ذات انابيب مزعنفة لكل من المبخر و المكثف كمنظومة تقطير.

تم بناء جهاز تقطير مختبري يستخدم الماء كمائع تشغيل وضع النموذج الرياضي لكلا الدورتين ومن تم تم بناء برنامج حسابي لتمثيل عمليات المنظومة خلال عملها في الحالة المستقرة. تم بناء برنامج متكامل لحساب خواص البخار ووضع كبرنامج فرعي للبرنامج الرئيسي. هذا البرنامج الفرعي يعمل ضمن مدى درجة حرارة (60 – 120)م^{o} و ضغط (0.199 – 1.985) جو. النتائج العملية اظهرت توافقا جيدا مع النتائج المستحصلة من البرنامج الحسابي. خلال عمل المنظومة في الحالة المستقرة، وجد إن معامل اداء دورة السيفون الحراري (موصلية الدورة) يزداد عندما يزداد معدل كتلة جريان مائع العمل و يزداد ايضا عندما يزداد ضغط مائع العمل و يصل إلى قيمة العظمى (493.022)واط/م^{٢}.كلفن عند كتلة جريان مائع العمل (5.5)كغم/ساعة، ضغط مائع العمل (0.8)جو و ضغط المائع الثانوي (1.01825)جو.

NOMENCLATURE

Symbol	Description	Units
A_b	Bare tube outside surface area	m^2
A_f	Fin surface area	m^2
$A_{i,o}$	Wall element outside area	m^2
A_o	condenser outer surface	m^2
C_p	Specific heat of constant pressure	kJ/(kg.K)
C_{sf}	Is an experimental constant **Yunis, A.C. & Micheal, A.B.[12]**	
C_v	Specific heat of constant volume	kJ/(kg.K)
d_h	Hydraulic diameter	m
g	Gravity acceleration	m/s^2
h	Enthalpy	kJ/kg
h_{1p}	Heat transfer coefficient of single-phase	$w/m^2.k$
h_{2p}	Heat transfer coefficient of two-phase	$w/m^2.k$
h_{amb}	Heat transfer coefficient of ambient temperature	w
H_{HE}	Height	m
h_o	Convection heat transfer for outer fluid	W/m^2
h_{pf}	Heat transfer coefficient of process fluid	w/m^2
i_{fg}	Latent heat of vaporization	J/kg
K_f	Thermal conductivity	w/m.k
L_{ft}	Length of fin	m
L_i	Distance along the evaporator or condenser from the entrance.	m
Pr_L	Liquid Prandtl number	
$P_{sat.}$	Saturation pressure	bar
P_w	Pressure	bar
q	Heat flux	w/m^2
Q_c	heat rejected by condenser	w
Q_i	heat transferred working fluid to wall element i	w
Re	Reynolds number.	
R_{pf}	Thermal resistance of process fluid side	W/m^2
R_w	Wall thermal resistance	W/m^2
R_{wf}	Thermal resistance of working fluid side	W/m^2
s	Entropy	kJ/kg
S	Parameter defined in eq. (36)	
T_{amb}	Ambient temperature	c^o
t_f	Fin thickness	m

T_{pf}	Temperature of process fluid	C^o
$T_{sat.}$	Saturation temperature	c^o
$T_{w,in}$	Inside wall temperature	C^o
$T_{w,o}$	Outside wall temperature	C^o
T_{wf}	Temperature of working fluid	C^o
U	Overall heat transfer coefficient	W/m.k
$\mathbf{U_{loop}}$	loop conductance	$w/m.c^o$
W_{ft}	Width of fin	m
W_{HE}	Width of heat exchanger	m
X	Quality	
α_{pf}	Ratio of the total heat transfer area to the total volume of the heat exchanger	m^{-1}
β_{pf}	Ratio of fin surface area to the total outside area	
$\Delta p_{frc.,1p}$	Pressure difference due friction	bar
η_f	Fin efficiency	
η_{tot}	Total fin efficiency	
θ	Inclination angle of the system pipes from horizontal	degree
ρ	Density	Kg/m^3
ρ_L	Liquid density	Kg/m3
ρ_v	Vapour density	Kg/m3
σ	Surface tension	N/m
v	Specific volume	M^3/kg
μ	Dynamic Viscosity	$N.s/m^2$
μ_L	Dynamic viscosity of liquid	$N.s/m^2$

1. INTRODUCTION

Thermosyphon are devices heated at locations below the points of cooling so that mass and heat transfer around the loop is transported through natural convection processes. In the presence of gravity, buoyancy forces due to thermal expansion of a working fluid guide the flow. Thus a circulation is created which transfers energy by convection from the heated section of the loop to the cooled one. The toroidal thermosyphon consists of a closed loop of tubing in the form of tours. The tube is filled with a fluid and heated over a part of its length and cooled over the other part. The steady and time dependent behavior of closed natural circulation loops is important for several engineering applications. For instance, in solar thermosyphon hot water heaters, the heat transfer fluid is heated at the solar collector and rises through a pipe to an elevated storage tank. Here, it transfers heat to the water in the tank, and consequently falls back down to the collector. Natural circulation may also arise in the emergency cooling of nuclear reactor cores, e.g., when a pump failure occurs. Other applications include cooling of internal combustion engines and turbine blades, geothermal power production, thermosyphon rebuilders, heat exchanger fins, permafrost protection, ice production, computer cooling, green houses, arctic and climate applications. **(Sh. H. Shams El-Din)**.

DESALINATION

Desalination is employed when:

1– There is a need for purification and reuse of water.

2– When long distance transport of fresh water is not feasible.

3– In arid and semi – arid areas, or when there is a source of saline water.

4– A direct or indirect source of energy is available.

Desalination describes a range of processes which are used to reduce the amount of dissolved solids in water. As a means of producing potable water, desalination is usually an expensive option. It is often associated with electricity generation plants, from which both electricity and waste heat are available (**Smith, M. and Shaw, R**).

Desalination processes are classified according to the salt separation phenomenon involved in the process, as follows:

1 - Processes Utilizing Membranes and Ion Selective Properties

In these processes, desalination is realized by using selective membranes, as in (Reverse Osmosis, Electrodialysis, Ion – Exchange and Solvent Extraction).

2 - Processes Employing the Phase Change of Water

In these processes, desalination occurs by (Crystallization Separation or Distillation).

DESALINATION BY DISTILLATION

Distillation is the oldest and most commonly used method of desalination. The world's first land-based desalination plant, a multiple-effect distillation (MED) process plant that had a capacity of 60 m^3/day, was installed on Curaçao, Netherlands Antilles, in 1928. Further commercial development of land-based seawater distillation units took place in the late 1950s, and initially relied on the technology developed for industrial evaporators (such as sugar concentrators) and for the shipboard distillation plants which were built during World War II. The multistage-flash (MSF), MED, and vapor-compression (VC) processes have led to the widespread use of distillation to desalinate sea water **(Al – Wakil, B.K).**.

TECHNICAL DESCRIPTION

Distillation is a phase separation method whereby saline water is heated to produce water vapor, which is then condensed to produce freshwater. The various distillation processes used to produce potable water, including MSF, MED, VC, and waste-heat evaporators, all generally operate on the principle of reducing the vapor pressure of water within the unit to permit boiling to occur at lower temperatures, without the use of additional heat. Distillation units routinely use designs that conserve as much thermal energy as possible by interchanging the heat of condensation and heat of vaporization within the units. The major energy requirement in the distillation process thus becomes providing the heat for vaporization to the feed water.

THE DOUBLE DISTILLATION HEAT PUMP SYSTEM:

The double – cycle distillation system is a new method for producing potable water. One such system was presented at **the committee of technology transfer conference**, by the name of **Zyclodest plant** at 2001. **Zyclodest plant** is a special mechanical vapor compression method. In it the working fluid exists in a separate loop for the heat recovery. Thus, the product vapor, process fluid, is only contact with heat – exchangers and does not pass through the compressor and its rotating elements. The schematic diagram of this heat pump can be envisioned as shown in the **Fig. (1)**.

According to **Fig (1)**, the thermosyphon loop performance, loop conductance (**U**) **Abdul – Ghafour, G.R.**, as follows:

$$\text{Loop conductance} = \frac{\begin{matrix}\text{Heat transfer rate rejected} \\ \text{by the condenser}\end{matrix}}{\begin{bmatrix}\text{Condenser} \\ \text{outer surface} \\ \text{area}\end{bmatrix}\begin{bmatrix}\text{Source} - \text{Sink} \\ \text{temperature} \\ \text{difference}\end{bmatrix}} \quad (1)$$

$$U_{loop} = \frac{Q_c}{[A_{out}][T_{source} - T_{sink}]} \quad (2)$$

Where,
T_{source}: is the temperature at the evaporator inlet.
T_{sink}: is the temperature at the condenser inlet.

The double – cycle distillation heat pump plant consists of two main cycles; the water compression – expansion cycle, which called also the compression – expansion vapor (CEV) cycle, and the process cycle, or named the thermosyphon loop. Each of these cycles is described as follows:

COMPRESSION-VAPOR CYCLE

The compression – expansion vapor cycle consists of compressor, expansion device, and two heats – exchangers with interconnecting piping. One of the heat – exchangers submerged in a pool boiling liquid and represents a condenser coil, which is mounted at an angle of inclination of about 15 degree with respect to the horizontal so as to allow for condensate drainage. The other heat – exchanger is exposed to a collective vapor and represents an evaporator coil. The evaporator and the condenser are mounted at the same angle to simplify the construction.

Process Cycle (Thermosyphon Loop)

This cycle consists of three main parts with interconnecting piping, namely: evaporation chamber, intermediate (IM) zone and condensation chamber. A brief description of this cycle is as follows:

In the evaporation chamber (boiler), the evaporator coil submerged in a pool of water and the heat will transfer through the evaporator walls to the water in the pool. Due to this heat transferred, water will boil and the amount of evaporative mass depends on the amount of heat transfer.

The vapor will rise due to the difference in density to pass through the intermediate (IM) zone through corrugated channel- Steam rising from the tub bottom will carry the small droplets of water and get rid of them is on a path winding passage changes direction sharply, leading to the elimination of water droplets and the accompanying access to saturated vapor
-. This part is used to avoid mist flow, and then the vapor enters the condensation chamber as a saturated vapor.

In the condensation chamber, the condenser coil is exposed to the saturated vapor. Due to the heat transferred to the working fluid inside the condenser through the walls of the condenser, the vapor will condensate on the outside walls of the condenser. The condensate will exit from the condensation chamber and return to the evaporation chamber by the distillate water pump, by gravity, or the pressure difference.

The heat exchangers used for evaporator and condenser of the double – loop distillation heat pump system are finned tube heat exchangers, as shown in **Fig. (3)**.

2. THEORY

A mathematical model will be set for the two loops and a computational program will be developed to simulate the two loops during steady – state operation for knowing the effect of the working mass flow rate on the thermosyphon loop performance with different working and process fluid pressures.

Thus, the analysis, in this study, is concentrated for the thermosyphon loop components and the working and process fluid, as follows:

2.1 Physical Properties

2.1.1 Working and Process Fluid

The working and process fluids in both the CEV and process loops respectively are that of pure water. The properties of pure water as required for simulation can be divided into:

a. Thermodynamic Properties: which include (υ, h, s, Cp and Cv), obtained from **UK Steam Tables in SI Units**.

b. Transport Properties: which include (ρ, K, μ and σ), obtained from (**Schmidt, E).**

All the above thermodynamic and transport properties are calculated for the different flow types using standard table correlations, in the temperature range of (70 – 130) ^{o}C.

For saline water, the thermodynamic and transport properties are direct functions of temperature and degree of salinity and in some cases they are established based on comparison with the same properties for pure water. The essential empirical equations for these properties as a function of temperature and degree of salinity are obtained from **(Sh. H. Shams El-Din)**.

2.1.2 Walls and Insulation

The properties of the system materials and insulation are assumed constant. Also the thermal conductivity for insulation (glass wool), pipes (wrought iron), Fins and tubes of the heat exchangers (aluminum) and system body (galvanized plates) are obtained from **(ASHRAE handbook & Holman, J.P).**

2.2 Heat Transfer Analysis:

2.2.1 Modeling of Evaporation Chamber

A- Modeling of condenser:

Referring to **Fig (4)**, the heat transfer rate from the working fluid (vapor) to the process fluid (liquid) in an element (i) in the condenser is:

Q_i = convective heat transfer from working fluid to the the wall of element (i) = conduction heat transfer through the wall of element (i) = convective heat transfer from the wall of element (i) to the process fluid (3)

$$= \frac{T_{wf} - T_{w,in}}{R_{wf}} = \frac{T_{w,in} - T_{w,o}}{R_{w}} = \frac{T_{w,o} - T_{pf}}{R_{pf}} \tag{4}$$

$$= \frac{T_{wf} - T_{pf}}{R_{wf} + R_{w} + R_{pf}} \tag{5}$$

and,

$$(UA)_o = \frac{1}{R_{wf} + R_{w} + R_{pf}} \tag{6}$$

B- Outside Convective Thermal Resistance:

Liquid (process fluid) – side convective thermal resistance is given as **(Holman, J.P)**:

$$R_{pf} = \frac{1}{A_{i,o}\, h_o\, \eta_{tot.}} \tag{7}$$

Outside surface area of the heat exchanger is calculated for each element length as follows:

$$A_{i,o} = \alpha_{pf}\left(L_i\, W_{HE}\, D_{HE}\right) \tag{8}$$

C- Outside Heat Transfer Coefficient:

The heat transfer coefficient of the boiled water (process fluid) (h_o), is calculated using the correlation proposed by (**Rohsenow)**, as follows:

$$q = \mu_L\, i_{fg}\left[\frac{g\left(\rho_L - \rho_v\right)}{\sigma_L}\right]^{1/2}\left[\frac{Cp_L\left(T_w - T_{pf}\right)}{C_{sf}\, i_{fg}\, Pr_L}\right]^3 \tag{9}$$

So,

$$h_o = \frac{q}{\left(T_w - T_{pf}\right)} \tag{10}$$

D- Fin Analysis:

The total fin efficiency ($\eta_{tot.}$) is calculated from the following equation (**Sarsam, W.S.)** :

$$\eta_{tot.} = \frac{\text{total heat transfer from tube and fin surface}}{\text{maximum heat transfer from tube and fin surface}} \tag{11}$$

$$= \frac{h_{pf}\, A_b\left(T_{pf} - T_{o,w}\right) + h_{pf}\, A_f\, \eta_f\left(T_{pf} - T_{o,w}\right)}{h_{pf}\left(A_b + A_f\right)\left(T_{pf} - T_{o,w}\right)} \tag{12}$$

$$= \frac{A_b + A_f\, \eta_f}{A_b + A_f} = 1 - \beta_{pf}\left(1 - \eta_f\right) \tag{13}$$

For continuous fins, fin efficiency (η_f) is calculated using the following equation **(Holman, J.P)** :

$$\eta_f = \frac{\tanh\left(m\, H_f\right)}{m\, H_f} \tag{14}$$

Where,

$$m = \left[\frac{2\, h_o}{K_f\, t_f}\right]^{1/2} \tag{15}$$

The fin efficiency (η_f) is multiplied by (2), because there are two fins protrude from the same point at the outer – surface of the flat tube of the condenser, see Fig. (4).

E- Conduction Thermal Resistance

The thermal resistance due to conduction is given as (**Holman, J.P**):

$$R_w = \frac{t_{ft}}{A_{av}\, K_{ft}} \tag{16}$$

Where,

$$A_{av} = \frac{A_o - A_{in}}{\ln\left(A_o / A_{in}\right)} \tag{17}$$

$$A_o = 2\left(L_{ft} + W_{ft}\right) L_i \tag{18}$$

$$A_{in} = 2\left[\left(L_{ft} - t_{ft}\right) + \left(W_{ft} - t_{ft}\right)\right] L_i \tag{19}$$

F- Inside Convective Thermal Resistance:

The working fluid – side convective thermal resistance is given as:

$$R_{wf} = \frac{1}{h_{in} A_{in}} \tag{20}$$

Since the working fluid inlet to the condenser as superheated vapor flow, therefore, the heat transfer coefficient (h_{in}) is calculated according to the correlation proposed by (**Sieder** and **Tate)** , for laminar or turbulent fully developed hydrodynamic flow.

For laminar flow (Re < 2400),

$$h_{1p} = 1.24 \frac{K}{d_h}\left[\mathrm{Re}\,\mathrm{Pr}\,\frac{d_h}{L_i}\right]^{1/3}\left[\frac{\mu}{\mu_w}\right]^{0.14} \tag{21}$$

For turbulent flow (Re > 2400),

$$h_{1p} = 0.027 \frac{K}{d_h} \mathrm{Re}^{0.8}\,\mathrm{Pr}^{0.4}\left[\frac{\mu}{\mu_w}\right]^{0.14} \tag{22}$$

When the bulk fluid temperature reaches the saturation temperature, the two – phase flow (condensation) heat transfer coefficient (h_{2p}) of an inclined condenser is calculated from the following correlation (**Sarsam, W.S.**) :

$$h_{2p} = E\left[\frac{g K_L^3 \rho_L^2 i_{fg}}{\mu_L d_h \left(T_{sat.} - T_w\right)}\right]^{1/4} \tag{23}$$

Where,

$$E = 0.727 \qquad \text{for } 0 < \theta < 40^{o}$$
$$E = 0.727\left[\cos\left(\frac{\theta - 40}{50}\right)90\right]^{1/4} \qquad \text{for } 40 < \theta < 90^{o} \tag{24}$$

The condensate in an actual condensation process is cooled farther to some average temperature between saturation temperature ($T_{sat.}$) and wall temperature (T_w), releasing more heat in the process. Therefore, the actual heat transfer will be large. **(Rohsenow)** show that the cooling of the liquid below the saturation temperature can be accounted by replacing (i_{fg}) by the modified latent heat of condensation (i_{fg}^*), which defined as follows **(Yunus, A.C. and Michael, A.B.)** :

For saturated vapor at the condenser inside,

$$i_{fg}^* = i_{fg} + 0.68\, Cp_L \left(T_{sat.} - T_w\right) \tag{25}$$

For superheated vapor at the condenser inside,

$$i_{fg}^* = i_{fg} + 0.68\, Cp_L \left(T_{sat.} - T_w\right) + Cp_v \left(T_v - T_{sat.}\right) \tag{26}$$

2.2.2 Modeling of Interconnecting Piping:

The same equations used for condenser to calculate the inside convective thermal resistance, conduction thermal resistance of the pipes walls and also the inside heat transfer coefficient for vapor and liquid region are used. The outside heat transfer coefficient is calculated by equations of natural convection in air depending on the angle of incline of the line with the horizontal **Sarsam, W.S.** , as follows:

1 – For angle of inclination equals to zero.

$$h_{amb} = 1.24\left(T_{wf} - T_{amb}\right)^{1/3} \quad (27)$$

2 – For angle of inclination more than zero.

$$h_{amb} = 1.31\left(T_{wf} - T_{amb}\right)^{1/3} \quad (28)$$

2.2.3 Modeling of Intermediate Zone:

The inside convective and conduction thermal resistances and also the inside heat transfer coefficient for single – phase flow (vapor) are calculated using the same equations which used in the process of modeling of the condenser. The outside heat transfer coefficient ($h_{amb.}$) is calculated using the equations which used in the process of modeling of interconnecting piping.

2.2.4 Modeling of Expansion – Device

The process fluid (vapor) will expands when it passes through the expansion – device. The expansion process occurs at constant enthalpy (i = c).

2.2.4 Modeling of Condensation Chamber

The evaporator is mounted in a pool of the process fluid (vapor). Due to the heat transfer, the temperature of the vapor will decrease until the vapor condenses at the outside surface of the evaporator walls. Thus, the same equations used for condenser are used for the evaporator, with the following differences.

A- Outside Heat Transfer Coefficient

The outside condensation heat transfer coefficient is calculated by the following correlation **(Sh. H. Shams El-Din.)** :

For $Re_L < 1800$

$$h_o = 0.725\left[\frac{\rho_L\left(\rho_L - \rho_v\right) g\, K_L^3\, i_{fg}}{\mu_L\, d_h\left(T_v - T_w\right)}\right]^{1/4} \quad (29)$$

For $Re_L > 1800$

$$h_o = 0.725\, B\left[\frac{\rho_L\left(\rho_L - \rho_v\right) g\, K_L^3\, i_{fg}}{\mu_L\, d_h\left(T_v - T_w\right)}\right]^{1/4} \quad (30)$$

Where,

$$B = 1.23795 + 0.0353808\,(nr) - 0.00157035\,(nr)^2 \quad (31)$$

nr: is the number of tube rows of the heat exchanger.

B- Inside Heat Transfer Coefficient:

The working fluid inlet to the evaporator as two – phase flow, therefore, the two – phase heat transfer coefficient is calculated according to the correlation proposed by **(Chen)**, as follows:

$$h_{2p} = h_{con.} + h_b \quad (32)$$

$$h_{con.} = 0.023\left[\frac{G\,(1-X)\,d}{\mu_L}\right]^{0.8} Pr_L \,\frac{K_L}{d}\, F \tag{33}$$

$$h_b = 0.00122\left[\frac{K_L^{0.79}\, Cp_L^{0.45}\, \rho_L^{0.49}}{\sigma^{0.5}\, \mu_L^{0.29}\, i_{fg}^{0.24}\, \rho_v^{0.24}}\right](T_w - T_{sat.})^{0.24}\,(P_w - P_{sat.})^{0.75}\, S \tag{34}$$

Where,

$$F = 1 \qquad \text{when } \frac{1}{X_{t,t}} < 0.1$$
$$F = 2.35\left(\frac{1}{X_{t,t}} + 0.213\right)^{0.736} \qquad \text{when } \frac{1}{X_{t,t}} > 0.1 \tag{35}$$

$$S = \left(1 + 0.12\, Re_{2P}^{\;1.14}\right)^{-1} \qquad \text{for } Re_{2P} < 32.5$$
$$S = \left(1 + 0.42\, Re_{2P}^{\;0.78}\right)^{-1} \qquad \text{for } 32.5 < Re_{2P} < 70 \tag{36}$$
$$S = 1 \qquad \text{for } Re_{2P} > 70$$

$$\frac{1}{X_{t,t}} = \left(\frac{X}{1-X}\right)^{0.9}\left(\frac{\rho_L}{\rho_v}\right)^{0.5}\left(\frac{\mu_v}{\mu_L}\right)^{0.1} \tag{37}$$

$$Re_{2P} = \frac{G\,(1-X)\,d}{\mu_L}\, F^{1.25} \cdot 10^{-4} \tag{38}$$

The heat transfer coefficient outside the condensation chamber ($h_{amb.}$) is calculated using the same equations which are used in the process of modeling of interconnecting piping.

2.3 Hydrodynamic Analysis

Process Fluid – Side

For single – phase flow, the frictional pressure drop is calculated from the following relation **(Franzini, J.B. and Fennimore)**:

$$\Delta P_{frc,1p} = 4\, f\, \frac{L_i}{d_h}\, \frac{G^2}{2\,\rho} \tag{39}$$

Where, for single – phase laminar flow

$$f = \frac{16}{Re} \tag{40}$$

And, for single – phase turbulent flow

$$f = \frac{0.079}{Re^{0.25}} \tag{41}$$

The hydrostatic pressure drop for the process fluid is calculated from, **(Al – Wakil, B.K.)**:

$$\Delta P_h = \rho\, g\, L \sin(\theta) \tag{42}$$

Where,

ρ : is the density of the process fluid.

θ : is the angle of inclination of the system pipe.

Minor losses occurring due to the inlet and exit to the pipes and the existence of fitting, valves, elbows ….. etc., are evaluated using the data given by (**Franzini)** and (**Finnemore0**, for the loss factor (F^L). The following relation is used for the pressure losses:

$$\Delta P_{minor} = F^L \frac{G^2}{2\rho} \tag{43}$$

3. Description of the Experiment

This study is directed towards the investigation of the thermosyphon loop performance (loop conductance), as a process cycle, in double cycle distillation heat pump system with varying the distillation conditions.

4. EXPERIMENTAL SETUP

The double – cycle distillation heat pump system for desalination, utilizing water as the working and process fluid, is designed and constructed in accordance with the schematic diagram in **Fig. (5).**

The two – loops of the heat pump are a sealed system charged with a known mass of working and process fluid and work under different pressures. The two – loops are insulated in order to minimize heat flow to ambient. A pictorial view of the test rig is shown in **Fig. (6)**.

Experimental program was initiated to studying the influence of mass flow rate of the CEV loop on the thermosyphon loop performance, U_{loop}, with different working and process pressures.

The evacuating and charging the system are attained using two different points for CEV loop and four different points for thermosyphon loop, and a fifth point at the bottom of the liquid line is used to specify the level of the feed water in the evaporation chamber.

The heat exchangers used for the evaporator and condenser has an outside surface area of about (0.325 m^2).

The evaporation and condensation chambers are constructed with a shape coincide with the size and configuration of the condenser and the evaporator coils respectively. The (I.M) zone is constructed from three inclined channels in the space between the evaporation and the condensation chambers. A (600) watt water heater is installed in the evaporation chamber. This heater is used as start – heating to reach the raw water to the boiling degree at the beginning of the operation.

The liquid (distillated water) and vapor lines are constructed from 1/2 and 3/4 inch galvanized (wrought iron) pipes respectively. 3/4 inch gate valve is used as expansion device.

Distillated water is used as the working fluid in CEV loop since its a cheep, good and available working fluid. Its also used as process fluid in thermosyphon loop to facility the loop performance investigation.

5. INSTRUMENTATION AND CALIBRATION

5. 1. Temperature Measurement

Thermally sensitive resistors (Thermistors) are used to measure the working and process fluid temperatures in all parts of the test rig. The thermistors are connected to a selector switch. The selector switch is connected to a digital multi-meter (hp 3435A) with a sensitivity of 0.1 Ω. Calibration of thermistor is carried out with temperature range of (70 – 115) ^oC.

5. 2. Pressure Measurement

A pressure gages (vacuum pressure gage the two another from (1-3) bar), bourdon type, are calibrated and used to measure the pressure of working and process fluid at different points of the system.

5. 3. Water Flow Rate Measurement

An orifice -0.6d- plate is calibrated and used to measure the volumetric flow rate of water inside the compression – expansion vapor loop.

6. LEAK TESTS

Before starting up the test runs for the system, the leak tests are carried out for the two – loops of the system

7. SYSTEM INSULATION

In order to minimize the heat transfer with the surrounding, a glass wool sheets, with different thickness (1, 1.5, 2) cm, insulation covered by an aluminum foil are used to cover the all parts of the two – loops of the system, as shown in **Fig. (6)**.

8. RESULTS AND DISCUSSION

The performance of the thermosyphon loop working with different mass flow rate is defined as a loop conductance (U_{loop}), as follows:

$$U_{loop} = \frac{Q_c}{[A_{out}][T_{source} - T_{sink}]} = \frac{Q_c}{[T_2 - T_4]} \tag{44}$$

Where,

$$Q_c = \dot{m}\left(i_{out} - i_{in}\right) \tag{45}$$

i_{in}: is the enthalpy at the condenser inlet.
i_{out}: is the enthalpy at the condenser outlet.

The effect of working mass flow rate on the thermosyphon loop performance for different process fluid pressure is shown in **Fig (7)** to **Fig(9)** at different working fluid pressure.

For all figures, we can be observed that the loop performance (loop conductance) increases when the working mass flow rate increase, for all process fluid pressure except the pressure of 1.02825 bar at working fluid pressure of 0.7 bar. This behavior can be explained by; increasing the working mass flow rate lead to increasing the heat transfer by the condenser, therefore, the loop conductance is increased.

From **Fig (7)**, and referring to the general trend on the behavior of the loop conductance with the working mass flow rate for low working fluid pressure, i.e. at working fluid pressure of 0.7 bars, it is shown that for process fluid of 1.01825 and 1.02325 bars, the loop conductance increased when the mass flow rate increased. This explained by the fact that when the working mass flow rate increased the liquid – vapor column in the condenser will be increased. So that, the effective condenser heat transfer surface area is increased as well. Thus, the heat rejected by the condenser is increased and causes the loop conductance increasing. The above behavior of the loop conductance with the working mass flow rate is occurred for working fluid pressure of 0.75 and 0.8 bar for any process fluid pressure, as shown in **Fig.(8)** and **Fig.(9)** respectively.

Now, returning to **Fig.(7)**, and for process fluid pressure of 1.02825 bar, it is observed that increasing the working mass flow rate will increase loop conductance up to the point in which the curve reaches zero slop, i.e. maximum loop conductance, and then starts to decrease. This can be explained by; the fact that increasing the process fluid pressure will increase the outer heat transfer coefficient and then the heat rejected by the condenser is decreased although the liquid – vapor column is increased, but increasing the liquid – vapor column is wane with the process fluid pressure increasing. In addition the heat transfer decrease, the high source temperature, which occur at low working fluid pressure, i.e. at 0.7 bar, and reaches to about 109.36 ^{o}C, also lead to decrease the loop conductance.

9. CONCLUSIONS

1. A computational program was developed for simulating the steady – state operation of a double – cycle distillation heat pump system. The computed results were in good agreement with the experimental data obtained from the test rig, for the thermosyphon loop performance.

2. From the experimental results, it was concluded that the water represents an efficient working fluid and can provide reasonably accurate results for the double – cycle distillation heat pump system. In addition it is cheap and available.
3. Any increase in the working mass flow rate, for working fluid pressure of 0.75 and 0.8 bars even for 0.7 bar at process fluid pressure of 1.01825 and 1.02325 bar, will clearly increase the thermosyphon loop conductance.
4. The thermosyphon loop conductance, for working fluid pressure of 0.7 bars at process fluid pressure of 1.02825 bar, increases with increasing the working mass flow rate until it reach the maximum points and then starts to decrease.
5. The maximum loop conductance was seen to occur at a working mass flow rate of 5.5 kg/hr, working fluid pressure of 0.8 bars and process fluid pressure of 1.01825 bars.

ACKNOWLEDGEMENT

The experimental rig which built by **(H. Gh. AL – Hussaini)**, was used as a working test rig on which predictions of results are made.

REFERENCES:

Abdul – Ghafour, G.R. "Thermosyphon Loop Performance with Multiple Pipe Evaporator", M.Sc. Thesis, University of Baghdad, 1996.

Al – Wakil, B.K. "Parametric Study of the Two – Phase Thermosyphone System", M.Sc. Thesis, University of Baghdad, 1998.

ASHRAE handbook "Fundamentals Volume", New York, 2009.

Chen, J.C. "Correlation for Boiling Heat Transfer to Saturated Fluids in Convective Flow", Inst. Eng. Chem. Process Design and Development, Vol. 5, No. 3, PP. 322 – 329, 1966.

Committee of Technology "Zyclodest Distillation Plant" Germany, 2001.

Franzini, J.B. and Finnemore, E.J. "Fluid Mechanics with Engineering Applications", McGraw – Hill Book Company, 10th Edition, 2002.

Holman, J.P. "Heat Transfer", McGraw – Hill Book Company, 1989.

Rohsenow, W.M. "A Method of Correlating Heat – Transfer Data for Surface Boiling of Liquids", Trans. ASME, Vol. 74, PP. 969 – 976, 1952.

Sarsam, W.S. "The Performance of Thermosyphon System as a Heat Regenerator", M.Sc. Thesis, University of Baghdad, 1995.

Schmidt, E. "Properties of Water and Steam in SI Units", New York, 1981.

Sh. H. Shams El-Din. " Heat transfer characteristics of an inclined single-phase toroidal thermosyphon", Alexandria Engineering Journal, Vol. 44 (2005), No. 2, 157-171.

Sieder, E.N. and Tate, J.E. "Heat Transfer and Pressure Drop of Liquids in Tubes", Ind. And Eng. Chem., Vol. 28, No. 12, PP. 1429 – 1434, 1936.

Smith, M. and Shaw, R. "Desalination by Reverse Osmosis and Distillation", WEDC Loughborough University, 2002.

UK Steam Tables in SI Units, London: Edward Arnold (publishers) LTD., 1970.

Yunus, A.C. and Michael, A.B. "Thermodynamic an Engineering Approach", McGrow – Hill Book Company, 2006.

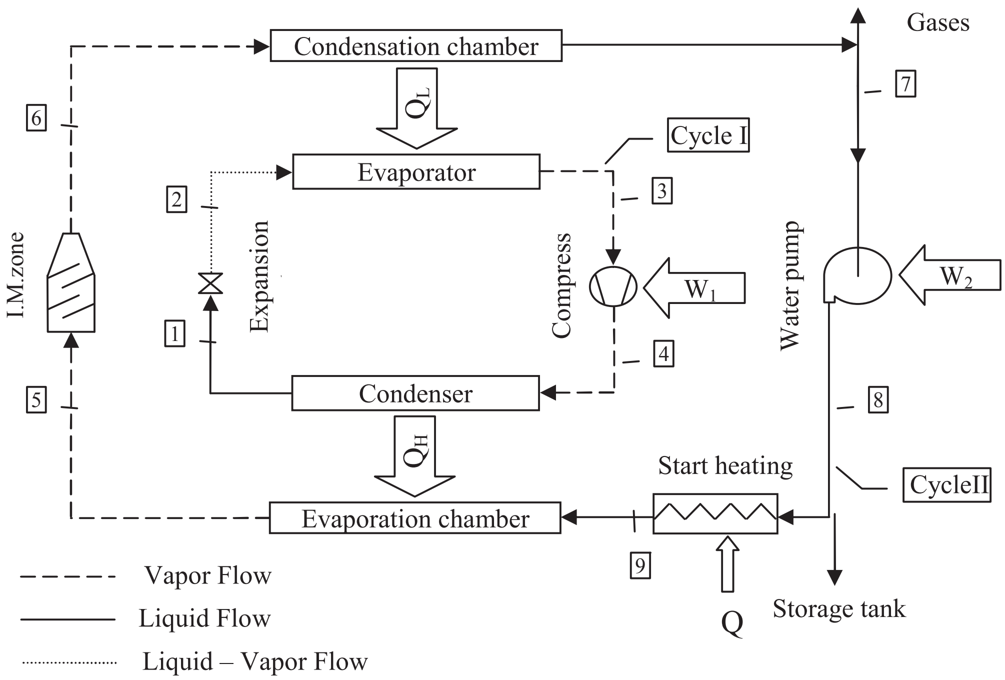

Cycle I : is the compression – expansion vapor cycle
Cycle II : is the process cycle

Fig. (1): Schematic diagram of hypothetical twine – cycle heat Pump.

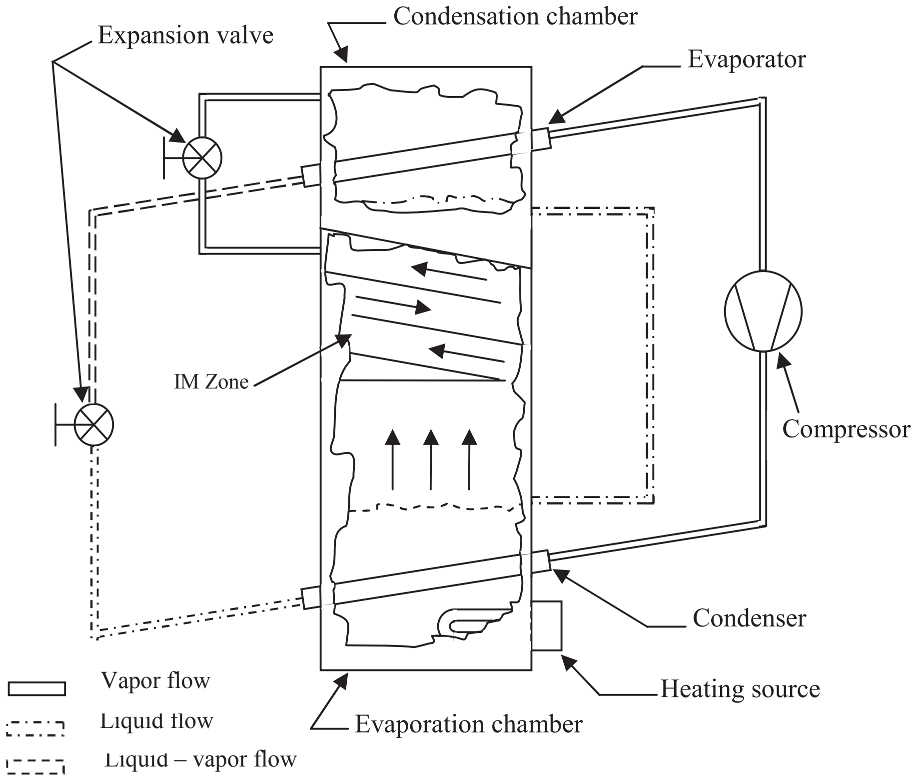

Fig. (2): Schematic representative diagram of the double – cycle distillation heat pump plant.

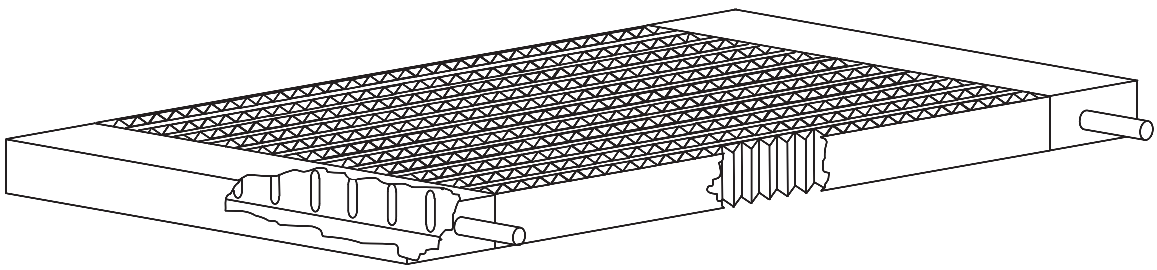

Fig. (3): Schematic diagram of the finned – tube heat exchanger used in this work for evaporator and condenser coils.

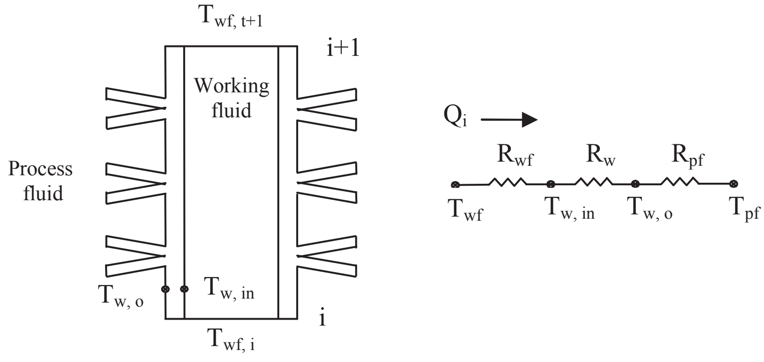

Fig. (4): Overall heat – transfer through an evaporator element
(a) sketch ; (b) thermal – resistance net work.

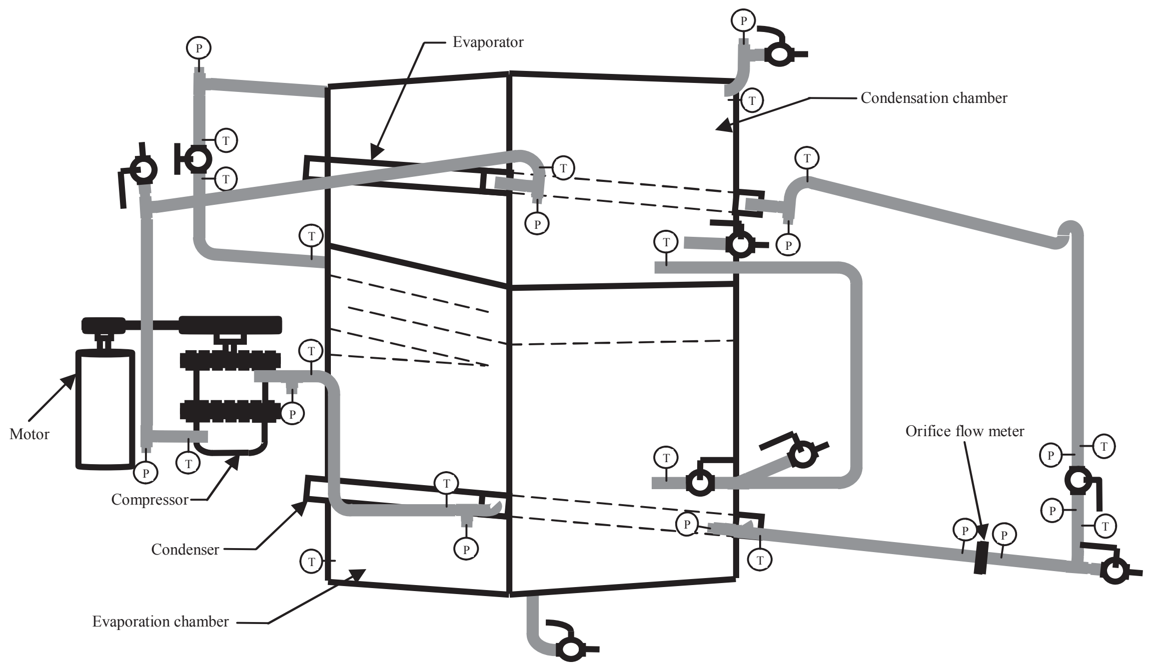

Fig. (5): P. I. Diagram of the test rig.

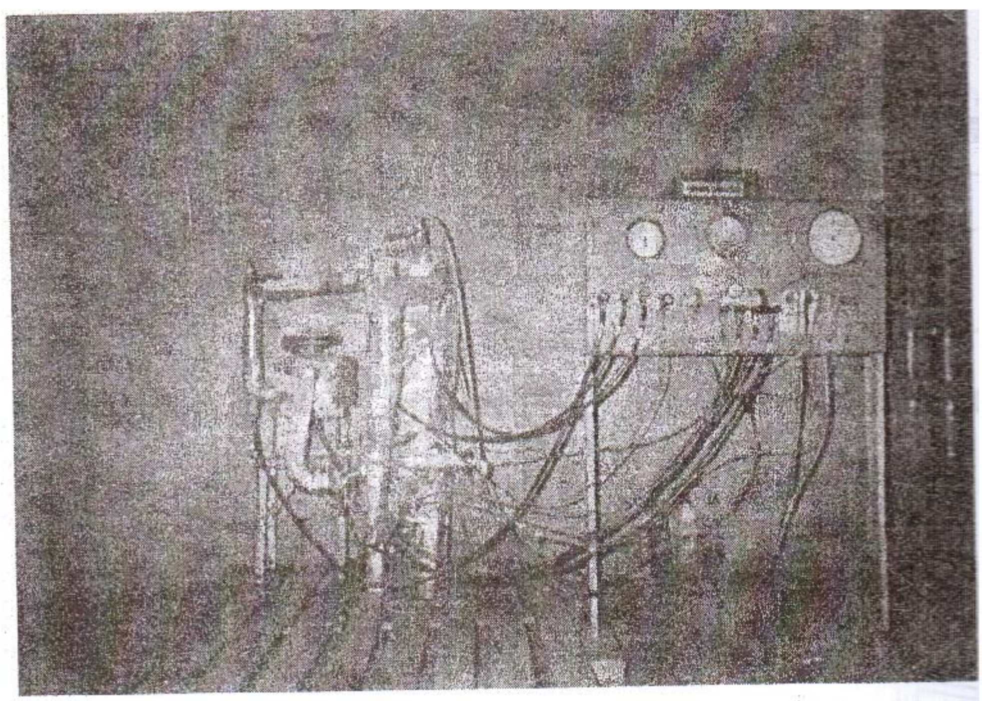

Fig. (6): Pictorial view of the test rig

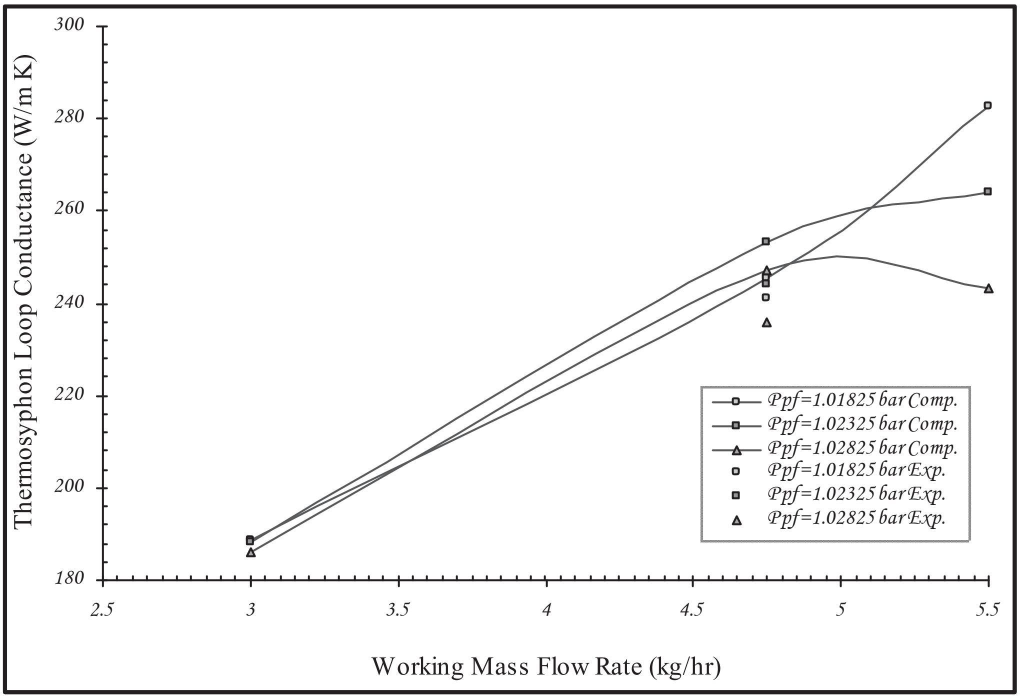

Fig. (7): Effect of working mass flow rate on the performance of the thermosyphon Loop for different process fluid pressure at working fluid pressure of 0.7 bars.

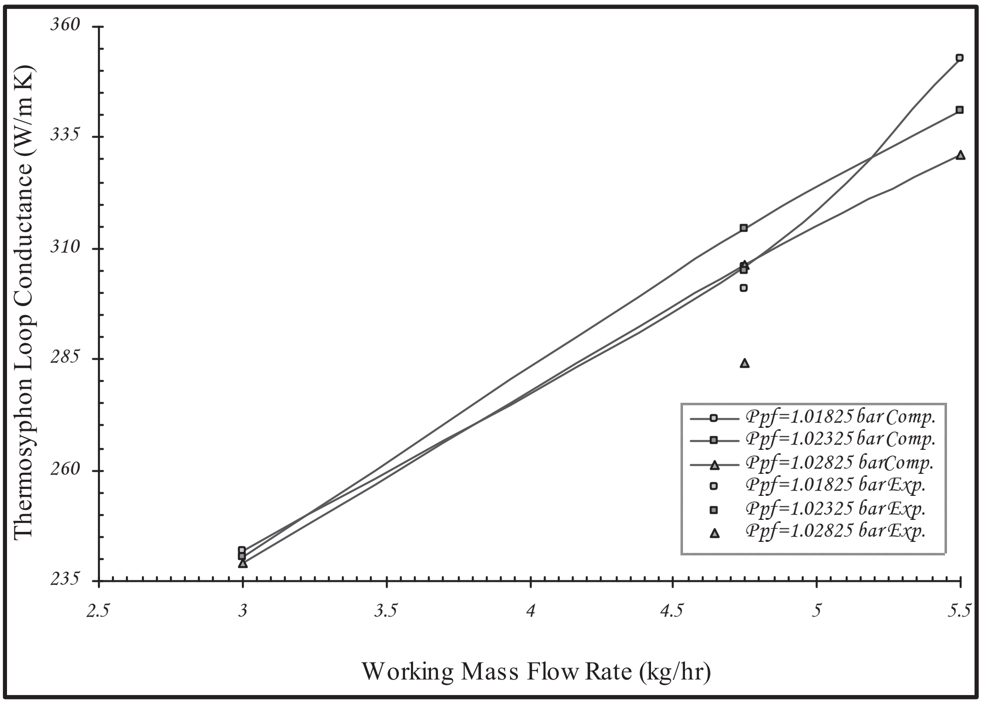

Fig. (8): Effect of working mass flow rate on the performance of the Thermosyphon Loop for different process fluid pressure at working fluid pressure of 0.75 bars.

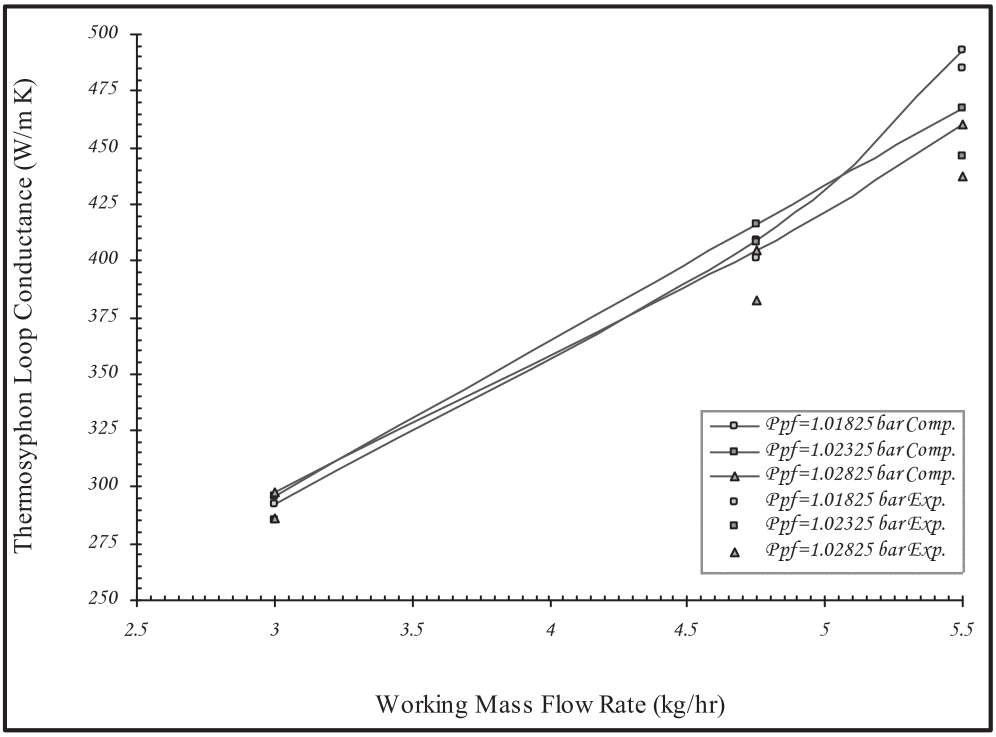

Fig. (9): Effect of working mass flow rate on the performance of the Thermosyphon loop for different process fluid pressure at working fluid pressure of 0.8 bars.